Eur. Phys. J. B **37**, 391–397 (2004)
DOI: 10.1140/epjb/e2004-00071-7

THE EUROPEAN PHYSICAL JOURNAL B

Formation and propagation of oscillating bubbles in DNA initiated by structural distortions

D. Hennig[a]

Freie Universität Berlin, Fachbereich Physik Institut für Theoretische Physik Arnimallee 14, 14195 Berlin, Germany

Received 7 August 2003 / Received in final form 31 October 2003
Published online 2 April 2004 –

Abstract. The initiation of the transcription process in DNA is linked with the dynamics originating from structural distortions of the double helix. It was proposed that such deformations might be caused by a 'hit and run' mechanism which is associated with the temporary attachment of some proteins, constituting activator factors, to regions of the DNA leaving it in deformed shape. In a nonlinear model approach we demonstrate that there exist such structural distortions of the double helix that appropriately serve to activate the formation of open regions in the form of oscillating bubble. The structure of the double helix form of DNA is modeled by a oscillator network model. We show that the underlying nonlinear dynamics supports localized solutions in the form of radial breathers and kink-shaped angular patterns. It is demonstrated that the radial breathers, which are attributed to localized H-bond deformations of the DNA molecule, move coherently along the double chain. We further illustrate that the breathers sustain the impact of heterogeneity due to the genetic code inscribed in DNA. Moreover, mobility of the breathers is also preserved when, the positions of the nucleotides are (randomly) modulated through fluctuational modes of the chemical environment, and energy dissipation due to non-elasticity damping of the motion of the nucleotides is incorporated. The amplitudes, oscillation periods and spatial extensions of the radial breathers resembles those found for the oscillating bubbles in real DNA molecules.

PACS. 87.15.-v Biomolecules: structure and physical properties – 63.20.Kr Phonon-electron and phonon-phonon interactions – 63.20.Ry Anharmonic lattice modes

The dynamical processes underlying biological activities of DNA are often not fully understood. A prominent example is represented by the transcription process for which the coding sequence on a DNA strand has to be made accessible to the RNA polymerase. This requests that hydrogen bonds connecting the two strands have to be (temporarily) broken so that the DNA strands separate. The open complex of DNA encloses 15−20 broken base pairs and is called the transcription bubble [1]. The formation of the transcription bubble and the initiation of its travel along the chain is associated with the action of proteins binding to specific regions of the DNA double helix (the promotor). In this context a 'hit and run' mechanism was suggested [2] on the basis of which the binding protein, operating as an activator factor, modifies structurally a region of the DNA for a short time and leaves the binding sites afterwards. In this way the activator factor might cause suitable local *structural deformations* that form the starting point for the creation of the transcription bubble. In addition, the latter should be able to move along the chain traversing so the genetic code. With the current study we aim to mimic the dynamics of the formation process of the opening complex in DNA originating from structural deformations. Regarding the opening process much attention has been paid to nonlinear models of the double helix [3,13]. The asset of utilizing nonlinear dynamics lies in the fact that there exist localized solutions, such as solitons and breathers, which can explain the strong localization of energy and the propagation of nonlinear excitations along the chain during the transcription process. In fact, for the Bishop-Peyrard (PB) model and its successors [6,9–12] moving localized excitations (breathers) have been found which reflect successfully some typical properties of the DNA opening dynamics such as the magnitude of the amplitudes and the time scale of the oscillating 'bubble' occurring prior to thermal denaturation.

We focus our interest on the initiation of the bubble formation process associated with initial structural deformations of the double helix. Our aim is to show that there exist indeed appropriate distortions constituting the source of dynamical processes such that nonlinear excitations develop matching the features of the experimentally observed oscillating bubbles. Such oscillating bubbles with their temporarily extended but yet unbroken H-bonds represent a first stage towards the creation of the transcription bubble for which in a region of the DNA double helix

[a] e-mail: hennigd@physik.fu-berlin.de

the H-bonds get broken so that the two strands are separated. The propagation of the transcription bubble along the DNA (in unison with the RNA-polymerase) renders the coding sequence of the gene accessible for the copy process.

In order to model the bubble formation and propagation in DNA the corresponding model incorporates the basic geometrical features of the Watson-Crick double helix. Following the approach in [9,10], we regard the double-stranded DNA as a network of coupled oscillators whose dynamics involves essential microscopic degrees of freedom of DNA. The main merit of such network model is that it is sufficiently complex to describe the mechanical behavior on the microscopic scale relevant for biomolecular processes. On the other hand, focusing on the most pertinent structural elements of the molecule, the model is of not too cumbersome form that the study of the corresponding dynamics is possible with acceptable computational efforts. Each of the oscillators of the network model represents a nucleotide. We abstract from the inner dynamical degrees of freedom of the nucleotides treating them as single nondeformable entities. This is justified on the grounds that the small-amplitude vibrational motions of the individual atoms are much faster than the relatively large-amplitude motions of the atom groups constituting the nucleotides [14]. A nucleotide is composed of a sugar, a phosphate and a base. The sugar-phosphate groups of neighboring nucleotides on the same strand are linked via covalent bonds establishing the rigid backbone to the strand. There is a base attached to every sugar. Two bases on opposite strands are linked via hydrogen bonds holding the two strands of DNA together.

The equilibrium positions of our DNA oscillator network model reproduce the geometrical features of B-DNA (see also [9,10,13]). The z-axis of the coordinate system coincides with the central helix axis. The base pairs are arranged in planes perpendicular to the central helix axis and the vertical distance between two consecutive planes is given by h. The equilibrium positions of the nucleotides are denoted by the coordinates $x_{n,i}^{(0)}$, $y_{n,i}^{(0)}$ and $z_{n,i}^{(0)}$. The index pair (n,i) labels the nth base on the ith strand with $i = 1, 2$ and $1 \leqq n \leqq N$, where N is the number of base pairs considered. The equilibrium distance between two bases within a base pair, d_0, is determined by

$$d_0 = \sqrt{(\,d_n^x\,)^2 + (\,d_n^y\,)^2}\,, \tag{1}$$

where $d_n^x = x_{n,1}^{(0)} - x_{n,2}^{(0)}$ and $d_n^y = y_{n,1}^{(0)} - y_{n,2}^{(0)}$ are the projections of the line connecting the two bases on the x, y-axes of the coordinate system.

Variations of the equilibrium value d_0 caused by displacements of the bases, $x_{n,i}$, $y_{n,i}$ and $z_{n,i}$, from their equilibrium positions are given by

$$d_n = \sqrt{(d_n^x + x_{n,1} - x_{n,2})^2 + (d_n^y + y_{n,1} - y_{n,2})^2 + (z_{n,1} - z_{n,2})^2} - d_0. \tag{2}$$

The distance variable $d_n(t)$ is hereafter also referred to as the radial variable because $d_n(t)/2$ represents actually the local helix radius. Each base is rotated around the central axis such that the relative twist between two consecutive base pairs is given by an angle θ_0. For later use we introduce the quantity

$$\theta_n = \arctan\frac{d_n^x + x_{n,1} - x_{n,2}}{d_n^y + y_{n,1} - y_{n,2}} + 2m\pi\,, \tag{3}$$

as the angle between the x-axis (as the reference direction) and the line connecting two (displaced) bases of a base pair measuring the alignment of the associated H-bridge. m is an integer to assure monotonicity of θ_n with respect to n.

The equilibrium distance between two adjacent bases on the same strand is given by

$$l_0 = \sqrt{h^2 + \left(x_{n,i}^{(0)} - x_{n-1,i}^{(0)}\right)^2 + \left(y_{n,i}^{(0)} - y_{n-1,i}^{(0)}\right)^2}, \tag{4}$$

and deviations from l_0 are determined by

$$l_{n,i} = \Big\{h^2 + \left(L_{n,i}^x + x_{n,i} - x_{n-1,i}\right)^2 + \left(L_{n,i}^y + y_{n,i} - y_{n-1,i}\right)^2 + \left(h + z_{n,i} - z_{n-1,i}\right)^2\Big\}^{1/2} - l_0. \tag{5}$$

The hydrogen bonds within a base pair are modeled typically by a Morse potential

$$U_h = D_n\left[\exp\left(-\frac{\alpha}{2}\,d_n\right) - 1\right]^2, \tag{6}$$

where the vibrations of d_n describe dynamical deviations of the hydrogen bonds from their equilibrium lengths d_0. The site-dependent depth of the Morse potential, D_n, depends on the number of involved hydrogen bonds for the two different pairings in DNA, namely the G-C and the A-T pairs. The former pair includes three hydrogen bonds while the latter includes only two. α is the range parameter.

The potential of the comparatively strong and rigid covalent bonds between the nucleotides n and $n-1$ on the ith strand is given by

$$U_c = \frac{K}{2}\,l_{n,i}^2, \tag{7}$$

where K is the elasticity coefficient.

With a further potential term, V_s, stacking effects are taken into account which impede that, due to the backbone rigidity, one base slides over another [1]. For the form of V_s we adopt the one used in [12]

$$V_s = \frac{S}{2}\,(d_{n,i} - d_{n-1,i})^2. \tag{8}$$

The presumably small longitudinal helix deformations can be modeled by a harmonic elasticity potential term given by

$$V_l = \frac{C}{2}\,(z_{n,i} - z_{n-1,i})^2. \tag{9}$$

The kinetic energy of a nucleotide is determined by

$$E_{kin} = \frac{1}{2m}\left[\left(p_{n,i}^{(x)}\right)^2 + \left(p_{n,i}^{(y)}\right)^2 + \left(p_{n,i}^{(z)}\right)^2\right], \qquad (10)$$

where m is the mass and $p_{n,i}^{(x,y,z)}$ denote the (x,y,z)-component of the momentum.

Our model Hamiltonian is then given by

$$H = \sum_{i=1,2}\sum_{n=1}^{N} E_{n,i}\,, \qquad (11)$$

with the on-site energy

$$E_{n,i} = E_{kin} + V_c + V_h + V_l + V_s\,, \qquad (12)$$

and the summation in (11) is performed over all nucleotides.

As the influence of the fluctuational vibrations of the aqueous environs on the vibrational dynamics of the DNA double-helix is concerned, it is simply expressed in additional terms in the Hamiltonian

$$\begin{aligned} H_{env} = &\sum_{i=1,2}\sum_{n=1}^{N}\left(\gamma_{n,i}^{(x)}\,\cos(\omega_{n,i}^{(x)}\,t + \delta_{n,i}^{(x)})\,x_{n,i}\right) \\ &+ \sum_{i=1,2}\sum_{n=1}^{N}\left(\gamma_{n,i}^{(y)}\,\cos(\omega_{n,i}^{(y)}\,t + \delta_{n,i}^{(y)})\,y_{n,i}\right) \\ &+ \sum_{i=1,2}\sum_{n=1}^{N}\left(\gamma_{n,i}^{(z)}\,\cos(\omega_{n,i}^{(z)}\,t + \delta_{n,i}^{(z)})\,z_{n,i}\right), \end{aligned} \qquad (13)$$

including temporal (harmonic) modulations of the positions of the nucleotides. $\gamma_{n,i}^{(x,y,z)}$ are the couplings strengths, $\omega_{n,i}^{(x,y,z)}$ and $\delta_{n,i}^{(x,y,z)}$ are the frequencies and phases. Incoherence of the modulation of the positions of the nucleotides induced by the fluctuations of the solvent is taken into account by site-depending coupling strengths, frequencies and phases. Particularly, the frequencies are arranged around a mean value and are simulated as independent random quantities distributed in an interval $[\,\bar{\omega} - \Delta\omega, \bar{\omega} + \Delta\omega\,]$ and the arbitrary phases are randomly distributed in the interval $[0, 2\pi)$. Typical frequencies of the environmental modes are of the order of $\bar{\omega} \leq 10^{-11}$ s^{-1}, that is at least one order of magnitude below the characteristic frequencies of H-bonds vibrations [15]. Moreover, the frequency range of the modes is also governed by the temperature of the system, viz. the DNA-chain and its aqueous surrounding, due to an Arrhenius-type temperature dependence, $\omega_T = \omega\,\exp(-E_a/k_bT)$ [15] with activation energy $\lesssim 6.9$ kcal/mol and prefactor of $\sim$0.6 THz [15].

With regard to specific parameter values we note that the geometrical parameters of the equilibrium configuration are well known [1]. The rotation angle for the twisted configuration is $\theta_0 = 36°$, the distance between base pair planes is $h = 3.4$ Å, and the inter-base distance (the diameter of the helix) is $d_0 = 20$ Å. For the average mass of one nucleotide we use $M = 4.982 \times 10^{-25}$ kg. Notice that the mass difference between the two possible base pairs in DNA is negligible whereas with respect to the H-bond coupling strength the two pairs are quite distinct, viz. the G-C bases couple with as nearly twice the strength as the A-T bases. In our model the DNA heterogeneity (the arbitrary base pair sequence) is reflected in randomly distributed bi-valued H-bond coupling strengths D_0 (for A-T) and $D_1 = 2\,D_0$ (for G-C). Consequently, due to the aperiodic arrangement of the two different basepairs, coding the genetic information, the DNA chain is of *A-B-disorder* type. Following Barbi et al. [9] we set $\alpha = 4.45$ Å^{-1}, $D_0 = 0.04$ eV, and $K = 1.0$ eV Å^{-2}. Concerning the parameters C and S there is little experimental evidence from which an estimate of them could be inferred. In [12] the value of the parameter S has been set to $S = 2K$ which we adopt here. (Alternatively, in a model approach of DNA denaturation dynamics [10] the parameters S and C were specified to fit the melting temperature of certain DNA polymers.) A plausible value for C is given by $C = S/10$ [13].

When the time is scaled as $t \to \sqrt{D_0\alpha^2/m}\,t$ one passes to a dimensionless formulation with quantities:

$$\tilde{x}_{n,i} = \alpha x_{n,i}, \tilde{y}_{n,i} = \alpha y_{n,i},\ \tilde{z}_{n,i} = \alpha z_{n,i} \qquad (14)$$

$$\tilde{p}_{n,i}^{(x)} = \frac{p_{n,i}^{(x)}}{\sqrt{mD_0}},\ \tilde{p}_{n,i}^{(y)} = \frac{p_{n,i}^{(y)}}{\sqrt{mD_0}},\ \tilde{p}_{n,i}^{(z)} = \frac{p_{n,i}^{(z)}}{\sqrt{mD_0}}, \qquad (15)$$

$$\tilde{D}_1 = \frac{D_1}{D_0},\ \tilde{C} = \frac{C}{\alpha^2 D_0},\ \tilde{K} = \frac{K}{\alpha^2 D_0},\ \tilde{S} = \frac{S}{\alpha^2 D_0}, \qquad (16)$$

$$\tilde{d}_n = \alpha\,d_n,\ \tilde{r}_0 = \alpha\,r_0,\ \tilde{h} = \alpha\,h, \qquad (17)$$

$$\tilde{\gamma}_{n,i}^{(x)} = \frac{\gamma_{n,i}^{(x)}}{\alpha D},\ \tilde{\gamma}_{n,i}^{(y)} = \frac{\gamma_{n,i}^{(y)}}{\alpha D},\ \tilde{\gamma}_{n,i}^{(z)} = \frac{\gamma_{n,i}^{(z)}}{\alpha D}, \qquad (18)$$

$$\tilde{\omega}_{n,i}^{(x)} = \frac{\omega_{n,i}^{(x)}}{\sqrt{D_0\alpha^2/m}},\ \tilde{\omega}_{n,i}^{(y)} = \frac{\omega_{n,i}^{(y)}}{\sqrt{D_0\alpha^2/m}},$$

$$\tilde{\omega}_{n,i}^{(z)} = \frac{\omega_{n,i}^{(z)}}{\sqrt{D_0\alpha^2/m}}. \qquad (19)$$

Subsequently, the tildes are dropped.

The equations of motion read as

$$\dot{x}_{n,i} = p_{n,i}^{(x)}\,, \qquad (20)$$

$$\begin{aligned} \dot{p}_{n,i}^{(x)} = &\,2D_n\,[\exp(-d_n) - 1\,]\,\exp(-d_n)\,\frac{\partial d_n}{\partial x_{n,i}} \\ &- 2K\left[\,l_{n,i}\frac{\partial l_{n,i}}{\partial x_{n,i}} + l_{n+1,i}\frac{\partial l_{n+1,i}}{\partial x_{n,i}}\,\right] \\ &+ S\,[\,d_{n+1} - 2\,d_n + d_{n-1}\,]\,\frac{\partial d_n}{\partial x_{n,i}} \;-\; \beta p_{n,i}^{(x)} \\ &- \gamma_{n,i}^{(x)}\,\cos\left(\omega_{n,i}^{(x)}\,t + \delta_{n,i}^{(x)}\right), \end{aligned} \qquad (21)$$

$$\dot{y}_{n,i} = p_{n,i}^{(y)}\,, \qquad (22)$$

$$\dot{p}_{n,i}^{(y)} = 2D_n\,[\exp(-d_n)-1\,]\,\exp(-d_n)\,\frac{\partial d_n}{\partial y_{n,i}} - 2K\left[\,l_{n,i}\frac{\partial l_{n,i}}{\partial y_{n,i}} + l_{n+1,i}\frac{\partial l_{n+1,i}}{\partial y_{n,i}}\,\right] + S\,[\,d_{n+1}-2\,d_n+d_{n-1}\,]\,\frac{\partial d_n}{\partial y_{n,i}} - \beta p_{n,i}^{(y)} - \gamma_{n,i}^{(y)}\,\cos\left(\omega_{n,i}^{(y)}\,t+\delta_{n,i}^{(y)}\right), \tag{23}$$

$$\dot{z}_{n,i} = p_{n,i}^{(z)}, \tag{24}$$

$$\dot{p}_{n,i}^{(z)} = 2D_n\,[\exp(-d_n)-1\,]\,\exp(-d_n)\,\frac{\partial d_n}{\partial z_{n,i}} - 2K\left[\,l_{n,i}\frac{\partial l_{n,i}}{\partial z_{n,i}} + l_{n+1,i}\frac{\partial l_{n+1,i}}{\partial z_{n,i}}\,\right] + S\,[\,d_{n+1}-2\,d_n+d_{n-1}\,]\,\frac{\partial d_n}{\partial z_{n,i}} - \beta p_{n,i}^{(z)} - \gamma_{n,i}^{(z)}\,\cos\left(\omega_{n,i}^{(z)}\,t+\delta_{n,i}^{(z)}\right) - C\,(\,2\,z_{n,i}-z_{n+1,i}-z_{n-1,i}\,), \tag{25}$$

with the derivatives

$$\frac{\partial d_n}{\partial x_{n,i}} = \frac{(-1)^{i+1}\,(d_n^x + x_{n,1} - x_{n,2})}{d_n + d_0}, \tag{26}$$

$$\frac{\partial l_{n,i}}{\partial x_{n,i}} = \frac{L_x + x_{n,i} - x_{n-1,i}}{l_{n,i} + l_0}, \tag{27}$$

and the equivalent expressions for $\partial d_n/\partial y_{n,i}$, $\partial l_{n,i}/\partial y_{n,i}$, $\partial d_n/\partial z_{n,i}$ and $\partial l_{n,i}/\partial z_{n,i}$.

For a more realistic model of the vibrational dynamics of DNA we consider also the effect of friction, incorporating energy dissipation due to non-elasticity caused by the viscosity of the aqueous environs consisting of water and a variety of salts, which is described by the additional damping terms $-\beta p_{n,i}^{(x,y,z)}$ on the r.h.s. of equations (21, 23) and (25) and β is the damping strength, viz. the decay rate. The interaction between water and the nucleotides determining mainly the decay rate (or equivalently the life time of bond vibrations) is influenced generally by the amount of water around the DNA molecule, the ionic concentration of the solvent and temperature [15,16]. (Typically, the decay rate varies with temperature according to an Arrhenius-law, $\beta = \beta_0\,\exp[-E/k_bT]$.) With 'life times' on time scales ranging from 10 ps to 100 ps, being times which amount to hundreds of periods of bond vibrations in DNA, the damping constant lies in the range $\beta = [0.01, 0.1] \times 10^{12}\ \mathrm{s}^{-1}$.

The values of the scaled parameters are given by $K = 0.683$, $r_0 = 44.50$, $h = 15.13$ and $l_0 = 31.39$. One time unit of the scaled time corresponds to 0.198 ps of the physical time.

We study now the formation and propagation of bubbles in DNA. Concerning the formation process our aim is to demonstrate that there exist deformations of the helix structure which represent the starting point for the creation of H-bridge breather solutions (extending over 15−20 base pairs) reproducing the oscillating 'bubbles' observed for the DNA-opening process [12].

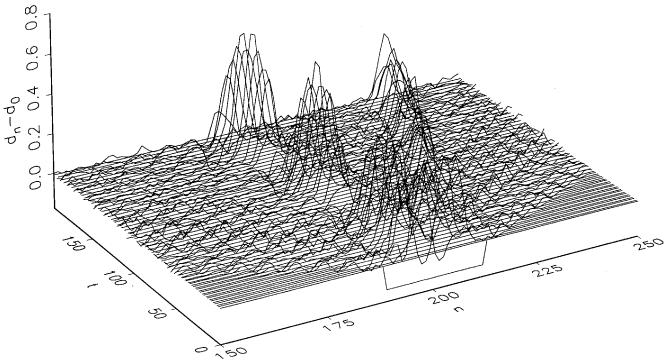

Fig. 1. The unperturbed case: Spatio-temporal pattern of the inter-base distance $d_n(t)$ in Å. For better illustration only a segment of the DNA lattice is shown. Parameters: $C = 0.126$, $K = 0.63$, $S = 1.26$, $D_0 = 1$, $D_1 = 2$ and $\gamma_{n,i}^{(x,y,z)} = \delta_{n,i}^{(x,y,z)} = 0$.

The dynamics of the opening process is dominated by the displacements of the bases in radial direction whose amplitudes typically exceed those of the angular displacements by at least one order of magnitude which reflects the backbone rigidity preventing larger twist deformations of the double helix [7]. Therefore, for the sake of simplicity, we assume that initially a number of consecutive sites in the center of the DNA lattice are exerted to forces acting in radial direction such that in this region the molecule experiences H-bond compressions. The distortion might be inflicted by the aforementioned 'hit and run' mechanism according to which a segment of the DNA is modulated structurally by the temporary action of some protein. These deformations are supposedly aligned along the orientation of the hydrogen bonds. Clearly, the distortions of the hydrogen bonds within a base pair are related with deformations of the covalent bonds of the adjacent region of the phosphate backbone. However, for the considered initial radial compressions of the order of $-0.30\ \text{Å} \leqslant d_n \leqslant -0.1\ \text{Å}$, the resulting deformations of the covalent bonds are inferior to the H-bond compressions.

We integrated the set of coupled equations (20–25) with a fourth-order Runge-Kutta method. For the simulation the DNA lattice consists of 400 sites and open boundary conditions were imposed. Before we embark on a study of the DNA dynamics including the coupling to environmental modes we investigate the *unperturbed* case for which the influence of the environmental modes and damping effects are discarded, i.e. $\gamma_{n,i}^{(x,y,z)} = 0$ and $\beta = 0$.

In Figure 1 we depict the spatio-temporal evolution of the distances, $d_n(t)$, between two bases of a base pair, which measures the variation of the length of the corresponding hydrogen bond expressed in Å. Initially, the twenty excited lattice sites have equally reduced radial amplitude yielding a localized rectangular pattern. Out of this non-equilibrium configuration, processes of energy redistribution set on. Most importantly, the vast majority of the excitation energy remains contained in localized radial patterns despite the dispersion of a small amount of excitation energy in the form of phonons in the rest of the DNA lattice. We observe that the localized

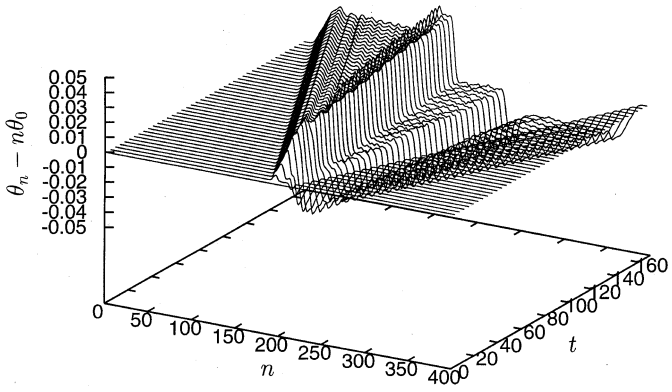

Fig. 2. The unperturbed case: Spatio-temporal pattern of the twist angle $\theta_n(t) - n\theta_0$ expressed in rad. Parameters as in Figure 1.

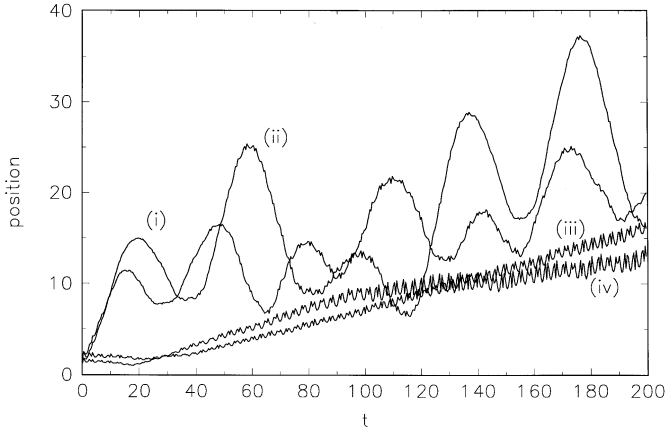

Fig. 3. Time-evolution of the breather center. Assignment of the curves: (i) Periodic case with parameters as in Figure 1 except for $\gamma_{n,i}^{(x,y,z)} = 0.01$, $\omega_{n,i}^{(x,y,z)} = 0.1$ and $\delta = 0.001$. (ii) Periodic case with parameters as in (i) except for decreased frequency $\omega_{n,i}^{(x,y,z)} = 0.08$. (iii) Unperturbed case with parameters as in Figure 1. (iv) Random case. Parameters as in (i) but with randomly distributed frequencies $[\bar{\omega} - \Delta\omega, \bar{\omega} + \Delta\omega]$ with mean value $\bar{\omega} = 0.1$ and interval width $\Delta\omega = 0.01$. Additionally the phases $\delta_{n,i}^{(x,y,z)}$ are randomly distributed in the interval $[0, 2\pi)$.

rectangular radial pattern is not preserved but gives way to the creation of new localized radial amplitude patterns. In fact, very rapidly two radial breathers are formed in the central region of the DNA lattice. These breathers even start to move in opposite directions in coherent fashion. Note that the stretching of a base pair distance is larger than the compression characteristic for the evolution in a Morse potential (see also [9]). Both breathers have nearly the same width comprising ten base pairs. However, the radial breather propagating towards the left end of the DNA lattice possesses larger amplitudes and moves faster than its counterpart traveling to the right.

In Figure 2 it is shown that the associated pattern of the deviations of the twist angles from their equilibrium values, $\theta_n(t) - n\theta_0$ expressed in rad, being initially overall zero, develops a local kink-like structure. Its plateaus continuously extend in either direction away from the central base pairs. In the course of time more and more base pairs become subject to angle deformations leading to a progressive untwisting of the helix. This untwisting of the helicoidal helix structure results from the coupling between the radial and the backbone degrees of freedom due to geometrical constraints and is typical for the DNA opening dynamics [9]. In contrast to the periodically oscillating pattern of the radial variable $d_n(t)$, corresponding to alternate stretchings and compressings of the hydrogen bonds, the torsional deformations $\theta_n(t) - n\theta_0$ adjust to a static deformation pattern.

With concern to the initial deformation pattern we remark that the dynamics does not change qualitatively when in addition to the radial compressions also angular deformations, being relevantly kink-shaped, are initially involved. Moreover, the initial radial compression pattern has not necessarily to be rectangular and also bell-shaped profiles having broad enough width lead to the formation of radial breathers that travel along the chain.

Taking into account the impact of the environmental modes and damping effects, i.e. $\beta \neq 0$ and $\gamma_{n,i}^{(x,y,z)} \neq 0$, we start our investigations with the case of coherent driving for which the frequencies and driving strengths have constant values $\gamma_{n,i}^{(x,y,z)} = \gamma$ and $\omega_{n,i}^{(x,y,z)} = \omega$ respectively (hereafter referred to as the *periodic* case). In addition there is no phase mismatch, i.e. $\delta_{n,i}^{(x,y,z)} = 0$. There arise at least two interesting questions; namely, will there still be radial breather solutions, and second, if so, will these breathers still travel coherently along the DNA lattice under the combined impact of driving and damping?

The results regarding the breather mobility are appropriately reflected in the time-evolution of the first momentum of the energy distribution given by

$$\bar{n}(t) = \sum_{i=1,2} \sum_{n=1}^{N} (n_c - n)\, E_{n,i}(t), \tag{28}$$

and the on-site energy $E_{n,i}$ is defined in equation (12).

This quantity describes the temporal behavior of the position(s) of the breather center(s) and hence, measures the mobility of the breathers. In general, the damped and periodically driven system behaves qualitatively like the formerly discussed unperturbed system, i.e. two counter-propagating breathers are produced. In addition, as the curves in Figure 3 reveal in the periodic cases (curves (i) and (ii)) the motion of the breather center gets periodically modulated by the driving modes indicated by the oscillations of $\bar{n}(t)$ around a straight line the slope of which determines the mean breather velocity.

Shown is the breather center evolution towards the left end of the DNA lattice. The corresponding plot of $\bar{n}(t)$ for the right-wards moving breathers exhibits equivalent features except for the lower amplitudes and velocities. Although in the periodic cases the path traveled over by the breather is not solely unidirectional the motion is, nevertheless, effectively directed towards the left end of the DNA lattice. The maximal amplitude of the oscillations

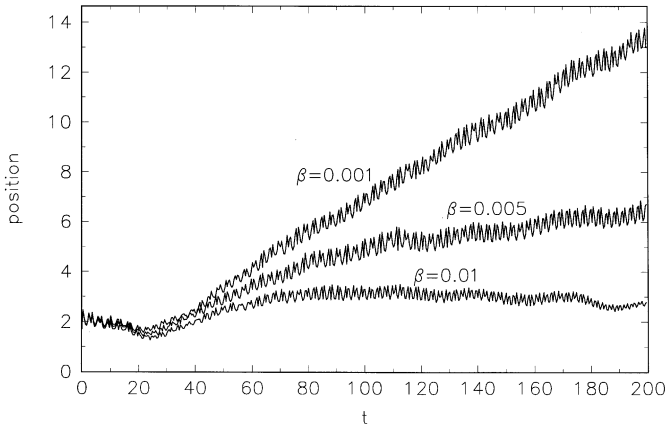

Fig. 4. Time-evolution of the (left) breather center in the damped and random case. Parameters as for the curve (iv) in Figure 3 except for varying damping strength β as indicated in the picture.

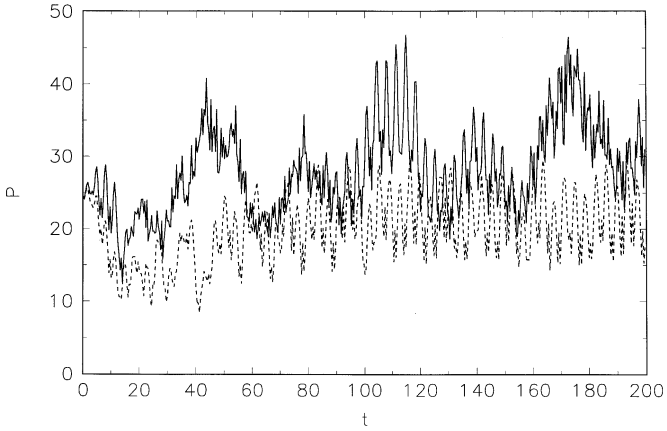

Fig. 5. Temporal behavior of the partition number. Periodic case (full line) and random case (dashed line) with parameters as for the curves (i) and (iv) in Figure 3 respectively.

of the breather center diminishes with rising driving frequency ω. When high enough driving frequency are chosen the motion of the breather center is presented by a straight line (apart from small-amplitude oscillatory deviations) restoring the unidirectional and straightforward character of the breather motion of the unperturbed case (curve (iii)).

For a more realistic study we assume that the frequencies of the fluctuating environmental modes are site-dependent leading to incoherent modulations of the positions of the nucleotides. More precisely, the frequencies are arranged around a mean value $\bar{\omega}$ (the indices are omitted) and are simulated as random quantities distributed in the interval $[\bar{\omega} - \Delta\omega, \bar{\omega} + \Delta\omega]$. Moreover, de-phasing of the environmental modes is assured by randomly distributed phases $\delta \in [0, 2\pi)$. Remarkably, in such *random* cases the system resembles virtually the behavior of the unperturbed system in the sense that the two created breathers propagate directedly and straightly in opposite directions towards either ends of the DNA lattice. From curves (iii) and (iv) in Figure 3 we infer that the breather in the random case moves effectively with slightly reduced velocity compared with its unperturbed counterpart. As the dependence on the random frequencies is concerned we observe no significant differences between the breather dynamics when the mean frequency $\bar{\omega}$ is varied in the relevant range of $(0, 0.1]$. Consequently, the breather velocity, width and amplitude appear to be unaffected by frequency changes. However, raising of the damping strength β has profound impact on the mobility of the breathers. In Figure 4 we show the time evolution of the breather center for three different values of β. Apparently, the larger β the less is the mobility of the breathers and for overcritical $\beta \gtrsim 0.01$ the motion towards the end(s) of the DNA lattice is inhibited by too strong non-elasticity. Apparently, then the energy losses cannot be compensated by the energy input provided by the external modes.

In order to quantify the degree of energy localization in the breathers we invoke the energetic partition number which is determined by

$$P(t) = \frac{(\sum_{i=1,2} \sum_{n=1}^{N} E_{n,i})^2}{\sum_{i=1,2} \sum_{n=1}^{N} E_{n,i}^2}. \tag{29}$$

The breather is completely confined at a single site if $P = 1$ and is uniformly extended over the lattice if P is of the order N, that is the number of lattice sites. Hence, P measures how many sites are excited to contribute to the radial breather pattern. We find that for the moving breathers in the periodic case the participation number grows in an initial interval and performs afterwards oscillations around a mean value corresponding to an increase of $P(t)$ typically by $\sim$20%. Distinctly, in the random case the partition number remains close to its initial value throughout the travel of the breathers along the DNA lattice (see Fig. 5). This points to improved energy storing capabilities in the random case compared with the periodic case. Moreover, it manifests how robust the localized amplitude patterns in the vibrational dynamics of DNA are with regard to random driving and friction. Equivalent results are obtained for the maintenance of localization in the case of the right-wards moving breather. Relating other features of the left and right breathers we note that in general the amplitudes of the former are by a factor of $\sim 1/3$ higher than the ones of the latter and the right breathers propagate with velocities being reduced by $\sim$20% compared with those of their left counterparts.

For further illustration of the bubble activation process we depict in Figure 6 the velocity of the left-wards moving breather as a function of the initial compression amplitude $d_n(0)$ (in the figure given with reversed sign) for a number of twenty distorted H-bonds. We investigated the dynamics including damping and random frequencies as well as random phases (details are given in the figure caption). Apparently, the stronger the H-bonds are initially compressed the faster travels the corresponding breather. The influence of the extension of the initially distorted DNA segment on the breather mobility is illustrated in Figure 7 showing the final position (base

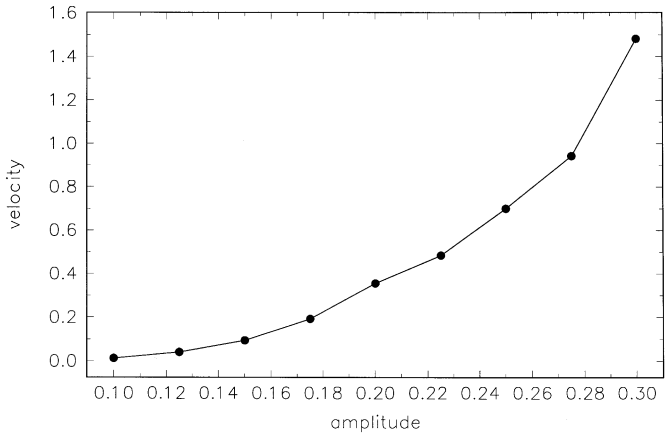

Fig. 6. Velocity of the left breathers (in Å/ps) as a function of the initial radial distortion $|d_n(0)|$ when twenty consecutive H-bonds are compressed. The frequencies of the driving modes are randomly distributed, $[\,\bar{\omega}-\Delta\omega,\bar{\omega}+\Delta\omega\,]$, with mean value $\bar{\omega}=0.1$ and interval width $\Delta\omega=0.001$. The phases $\delta_{n,i}^{(x,y,z)}$ are randomly distributed in the interval $[0,2\pi)$ and the damping parameter is $\beta=0.001$.

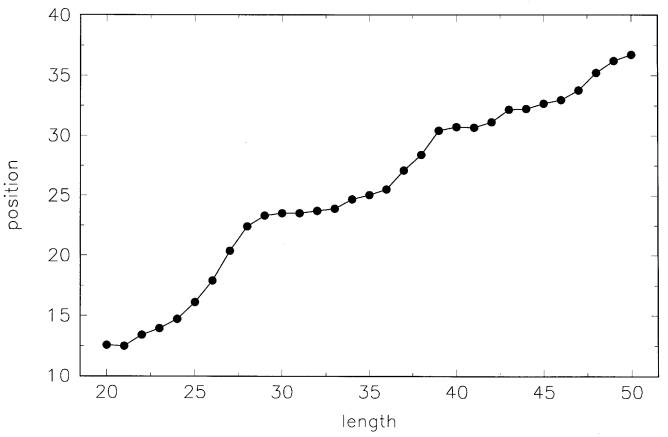

Fig. 7. Final position (base pair) of the left breather in dependence of the length of the initially compressed DNA region, viz. the number of distorted H-bonds. Initial compression amplitude $d_n(0)=-0.25$ Å.

pair) of the left breather as a function of the length of the initially compressed DNA region, viz. the number of distorted H-bonds with reductions $d_n(0)=-0.25$ Å. Interestingly, the broader the initial deformation radial pattern is the faster the localized breather related with the structure of the compressed radii propagates. We remark that the (mean) extension of the left-ward and right-ward moving breathers is virtually equal for both. In fact, either breather comprises (at most) half the number of the initially excited sites (compressed H-bonds) and we found that the broadest breathers comprise 23 base pairs which is in good agreement with the observation made for DNA, namely when enzymes interact with the promoter sites over a region of 50 base pairs the eventually formed open complex involves only 20 base pairs. The amplitudes of these breathers range from 0.1 Å to 0.3 Å which is of the order of the amplitudes of the experimentally observed oscillating bubbles. In addition, the frequencies of the breathers resemble those of the oscillating bubbles which are of the order of 7−21 THz.

In conclusion, we observed that out of an initial non-equilibrium situation, for which the hydrogen bonds of a segment of the DNA lattice have been compressed two counter-propagating breathers develop in the radial displacement variables. The shape of these breathers reproduces the oscillating bubbles observed to precede thermal denaturation of DNA. In particular a breather oscillates with periods in the range 0.3−0.8 ps and possesses average spatial extension over 10−20 base pairs and maximal amplitudes of the order of ∼0.3 Å. The breathers can combine and grow in amplitude and contribute so to the creation of the denaturation bubble.

Due to the coupling between the radial and the angular motions the angular displacement variables adopt a kink-like structure associated with unwinding of the helix. We demonstrated that the radial breathers sustain the combined impact of fluctuating environmental modes, modulating the positions of the nucleotides, and damping caused by non-elasticity effects. Remarkably, the moving breathers prove to be insensitive to DNA heterogeneity.

The author acknowledges support by the Deutsche Forschungsgemeinschaft via a Heisenberg fellowship (He 3049/1-1) and is indebted to E. Starikow for valuable discussions.

References

1. L. Stryer, *Biochemistry* (Freeman New York, 1995)
2. G. Rigaud, J. Roux, R. Pictet, T. Grange, Cell **67**, 977 (1991)
3. S.W. Englander, N.R. Kallenbach, A.J. Heeger, J.A. Krumhansl, S. Litwin, Proc. Natl. Acad. Sci. USA **777**, 7222 (1980)
4. S. Yomosa, Phys. Rev. A **27**, 2120 (1983); S. Yomosa, Phys. Rev. A **30**, 474 (1984)
5. M. Peyrard, A.R. Bishop, Phys. Rev. Lett. **62**, 2755 (1989)
6. T. Dauxois, M. Peyrard, A.R. Bishop, Phys. Rev. E **47**, 684 (1993)
7. L.V. Yakushevich, Quart. Rev. Biophys. **26**, 201 (1993); L.V. Yakushevich, *Nonlinear Physics of DNA* (Wiley and Sons, 1998)
8. G. Gaeta, C. Reiss, M. Peyrard, T. Dauxois, Riv. Nuovo Cim. **17**, 1 (1994)
9. M. Barbi, S. Cocco, M. Peyrard, Phys. Lett. A **253**, 358 (1999)
10. S. Cocco, R. Monasson, Phys. Rev. Lett. **83**, 5178 (1999)
11. M. Barbi, S. Cocco, M. Peyrard, S. Ruffo, J. Biol. Phys. **24**, 97 (1999)
12. M. Barbi, *Localized Solutions in a Model of DNA Helicoidal Structure*, Ph.D. thesis, Università degli Studi di Firenze (1998)
13. A. Jessica, D. Hennig, Physica A **323**, 519 (2003)
14. J.A. McCamon, S.C. Harvey, *Dynamics of Proteins and Nucleic Acids* (Cambridge Uni. Press, Cambridge, 1989)
15. E. Starikow, Phys. Rep. **264**, 89 (1997)
16. M.C.R. Symons, Cell. Mol. Life Sci. **57**, 999 (2000)